Formation and Optical Properties of Thin and Wide Tin-doped ZnO Nanobelts

Xiao-Sheng Fang,* Chang-Hui Ye, Li-De Zhang, Yan Li, and Zhi-Dong Xiao
Key Laboratory of Materials Physics, Institute of Solid Physics, Chinese Academy of Sciences, P. O. Box 1129, Graduate School of the Chinese Academy of Science, Hefei 230031, P. R. China

(Received January 5, 2005; CL-050018)

Thin and wide ZnO nanobelts doped with 5 atom % tin have been achieved under different flowing atmosphere. Photoluminescence measurements show a blue shift in the near band edge (NBE) emission spectrum compared to a bulk single crystal of ZnO and the intensity ratio of the NBE to the green emission of these Sn-doped ZnO nanobelts can be controlled by altering the flowing atmosphere.

One-dimensional (1D) nanostructures have received much attention owing to their potential interests for understanding fundamental physical concepts and for applications in constructing nanoscale electric and optoelectronic devices.[1] Zinc oxide (ZnO), a wide-band-gap semiconductor ($E_g = 3.37$ eV at room temperature), is currently undergoing a renaissance because of its many exciting properties. Pure ZnO nanowires, nanobelts, and nanotubes have been synthesized via a variety of techniques, such as template-assisted growth,[2] vapor–liquid–solid methods,[3] chemical vapor deposition,[4] and solution-based synthesis etc.[5]

Impurity doping is an effective method for manipulating the physical properties of semiconductors.[6] Recently, doping of the nanostructures has become an important issue for the more diverse range of applications.[7] So far as we know, Sn-doped 1D ZnO nanobelts have not been reported yet. In this article, thin and wide Sn-doped ZnO single-crystalline nanobelts were fabricated via chemical vapor deposition under different flowing atmosphere. A NBE band at 370 nm and a green emission band centered at 518 nm were obtained and the intensity ratio of the NBE to the green emission can be controlled by altering the flowing atmosphere.

Synthesis of Sn-doped ZnO nanobelts was carried out in a tube furnace. The high purity (99.99%) zinc powders (≈0.325 g) were placed in a ceramic boat. Then, this boat was inserted at the center of the horizontal alumina tube furnace. A tin-coated silicon wafer was placed downstream in the alumina tube. The system was rapidly heated to 700 °C in 5 min and kept at this temperature for 30 min in a flowing atmosphere [air (no flow), dry and humid argon (Ar) flow, and argon/oxygen (O_2) gas mixture]. During the heating process, the flow rate was kept at 100 sccm, water was introduced into the reaction by placing an alumina crucible with about 50 mL of distilled water in the upstream side of the alumina tube for humid Ar flow, and the ratio of the gases Ar/O_2 is 5:1 for Ar/O_2 gas mixture.

The as-synthesized products were characterized by X-ray diffraction [(XRD) X'Pert Pro MPD with Cu Kα radiation], scanning electron microscopy [(SEM) JEOL JSM 6700F], high-resolution transmission electron microscopy [(HRTEM) JEOL JEM2010FEF], and energy-dispersive X-ray spectroscopy (EDX). Photoluminescence (PL) spectra were obtained using an Edinburgh FLS 920 fluorescence spectrophotometer (Xe 900 lamp) at room temperature.

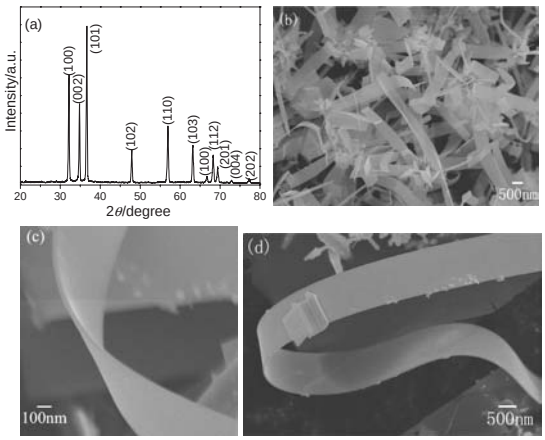

Figure 1. (a) XRD pattern of as-synthesized products; (b) a low-magnification SEM image (c) and (d) a high-magnification SEM images of a Sn-doped ZnO nanobelt, revealing the thin and wide shape characteristics of the nanobelt.

Figure 1a shows XRD pattern of the as-synthesized samples which were achieved under Ar flow. There is no diffraction signal originated from tin and its compounds in the XRD data and the diffraction peaks can be indexed to a hexagonal wurtzite-structured ZnO which means that the impurity does not change the wurtzite structure of ZnO. Figure 1b is a low-magnification SEM image of the synthesized Sn-doped ZnO nanobelts were achieved under Ar flow and it shows that large-scale Sn-doped ZnO nanobelts were formed. Figures 1c and 1d are the high-magnification SEM images of one Sn-doped ZnO nanobelt. They reveal that the nanobelt have the width of ≈800–1500 nm, the thickness of ≈20–60 nm, and have the length that ranges from several tens of microns.

Further structural characterization was carried out using TEM. Figure 2a shows an individual Sn-doped ZnO nanobelt with a width of ≈1400 nm and the nanobelt has a uniform width along its entire length. HRTEM and its correponding fast Fourier transform (FFT) studies will provide further insight into the microstructures of the nanobelts. As shown in Figure 2d, HRTEM image and its FFT (inset) show the nanobelt (Figure 2a) has a hexagonal wurtize structure and the nanobelt grows along $[2\bar{1}\bar{1}0]$ (the a axis), with its top/bottom surface $\pm$ (0001) and the side surfaces $\pm$ $(01\bar{1}0)$ (inset in Figure 2a). Most of the Sn-doped ZnO thin and wide nanobelts are single crystalline without dislocations and defects (Figure 2d), and its geometrical shape is uniform. However, planar defects are observed occasionally and dislocations are rarely seen. Figure 2b shows the TEM image and the corresponding HRTEM image (inset) of one Sn-doped ZnO nanobelt with a uniform distribution of planar defects along the entire nanobelt. EDX identifies that the composition of the nanobelts is Zn, O and Sn (Figure 2c). The

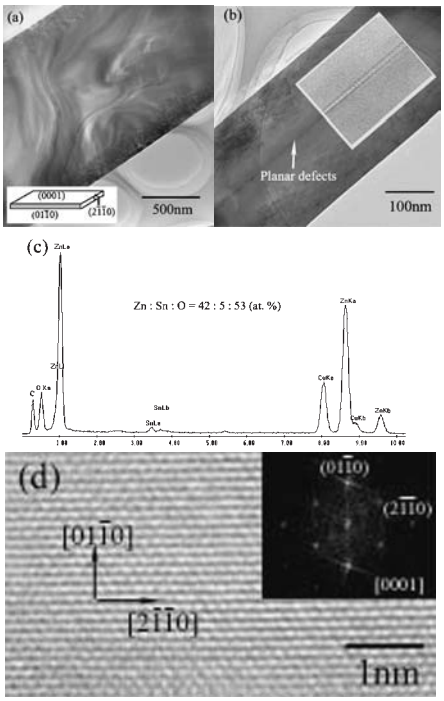

Figure 2. (a) and (d) a low magnification TEM image and the corresponding HRTEM image and its FFT recorded from a typical unselected Sn-doped ZnO nanobelt. The inset in (a) is the structure model of the Sn-doped ZnO nanobelts. (b) a uniform distribution of planar defects along the entire nanobelt is observed occasionally. (c) EDX data shows 5 atom % Sn.

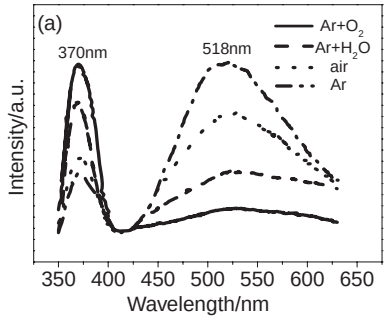

Figure 3. Photoluminescence spectra of Sn-doped nanobelts prepared under different flowing atmosphere.

Sn content is about 5 atom %. The Cu peaks come from the TEM grid.

Naturally in the ZnO growth, the highest growth rate is along the *c* axis and the large facets are usually {01$\bar{1}$0} and {2$\bar{1}\bar{1}$0}.[4a,8] Recently, Wang et al. reported that the controlled synthesis of free-standing ZnO nanobelts whose surfaces are dominated by the large polar surfaces and the nanobelts grow along the *a* axis by controlling growth kinetics.[9] In this article, we find that it is also possible to change the growth behavior of ZnO nanobelts by doping.

Figure 3 displays the room temperature PL spectra of the Sn-doped ZnO nanobelts prepared under different flowing atmosphere and the excitation wavelength was 325 nm. There are some differences both in structural and optical aspects between Sn-doped ZnO nanobelts and Sn-doped ZnO nanowires.[10]

The NBE emission peak of Sn-doped ZnO thin and wide nanobelts showed a blue shift (about 0.024 eV) compared to a bulk single crystal of ZnO. The blue shift of NBE emission is due to Burstein–Moss effect with an increasing in band-gap value which is due to tin doping.[11] The green emission band at 518 nm originates from the recombination of the holes with electrons occupying the singly ionized O vacancy.[12] The intensity ratio of the NBE to the green emission is determined by the concentration of O vacancy in the nanobelts; therefore, we are able to selectively enhance the NBE emission performance of these Sn-doped ZnO nanobelts by altering the synthesis parameters, such as the flowing atmosphere in the furnace, where a higher reaction activity and/or higher partial pressure of oxygen will decrease the concentration of O vacancy in the nanobelts.

In conclusion, Sn-doped ZnO thin and wide nanobelts (5 atom % Sn) were prepared through a simple chemical vapor deposition process. The PL apectra of the nanobelts shows that a NBE band at 370 nm and a green emission band centered at 518 nm and the intensity ratio of the NBE to the green emission of these Sn-doped ZnO nanobelts can be controlled by altering the flowing atmosphere. These Sn-doped ZnO nanobelts may be applied as detectors or UV light application devices.

We are grateful Anhui Provincial Natural Science Foundation (Grant number 03044905) for the support of this work.

References

1 J. T. Hu, T. W. Odom, and C. M. Lieber, *Acc. Chem. Res.*, **32**, 435 (1999).
2 a) Y. Li, G. W. Meng, L. D. Zhang, and F. Phillipp, *Appl. Phys. Lett.*, **76**, 2011 (2000). b) C. H. Liu, J. A. Zapien, Y. Yao, X. Meng, C. S. Lee, S. S. Fan, Y. Lifshitz, and S. T. Lee, *Adv. Mater.*, **15**, 838 (2003).
3 a) M. H. Huang, S. Mao, H. Feick, H. Q. Yan, Y. Y. Wu, H. King, E. Weber, R. Russo, and Y. P. Yang, *Science*, **292**, 1897 (2001).
4 a) Z. W. Pan, Z. R. Dai, and Z. L. Wang, *Science*, **291**, 1947 (2001). b) J. Q. Hu and Y. Bando, *Appl. Phys. Lett.*, **82**, 1401 (2003). c) X. H. Kong, X. M. Sun, and Y. D. Li, *Chem. Lett.*, **32**, 546 (2003).
5 a) L. Vayssieres, *Adv. Mater.*, **15**, 464 (2003). b) Y. N. Zhao and Y. U. Kwon, *Chem. Lett.*, **33**, 1578 (2004).
6 H. J. Chun, Y. S. Choi, S. Y. Bae, H. C. Choi, and J. Park, *Appl. Phys. Lett.*, **85**, 461 (2004).
7 a) S. Y. Bae, H. W. Seo, and J. Park, *J. Phys. Chem. B*, **108**, 5206 (2004). b) C. Ronning, P. X. Gao, Y. Ding, Z. L. Wang, and D. Schwen, *Appl. Phys. Lett.*, **84**, 783 (2004).
8 Z. R. Tian, J. A. Voigt, J. Liu, B. Mckenzie, and M. J. Mcdermott, *J. Am. Chem. Soc.*, **124**, 12954 (2002).
9 X. Y. Kong and Z. L. Wang, *Appl. Phys. Lett.*, **84**, 975 (2004).
10 S. Y. Li, P. Lin, C. Y. Lee, T. Y. Tseng, and C. J. Huang, *J. Phys. D: Appl. Phys.*, **37**, 2274 (2004).
11 A. Bougrine, A. El Hichou, M. Addou, J. Ebothe, A. Kachouane, and M. Troyon, *Mater. Chem. Phys.*, **80**, 438 (2003).
12 a) E. Burstein, *Phys. Rev.*, **93**, 632 (1954). b) F. K. Shan, B. I. Kim, G. X. Liu, Z. F. Liu, J. Y. Sohn, W. J. Lee, B. C. Shin, and Y. S. Yu, *J. Appl. Phys.*, **95**, 4772 (2004).

Published on the web (Advance View) February 23, 2005; DOI 10.1246/cl.2005.436